Q. J. R. Meteorol. Soc. (2005), **131**, pp. 1215–1232 doi: 10.1256/qj.03.220

On the Doppler effect in a transient gravity-wave spectrum

By MANUEL PULIDO*

Facultad de Ciencias Exactas y Naturales y Agrimensura, Universidad Nacional del Nordeste, Argentina

(Received 10 December 2003; revised 25 October 2004)

SUMMARY

The power-spectrum evolution of a transient gravity-wave disturbance propagating conservatively upwards in a shear flow is examined. It is proven that the wave action for a disturbance suffering Doppler shifting is invariant in the wave-number space. On the other hand, vertical wave-momentum flux, even when it is invariant for waves of fixed frequency, is not invariant in the wave-number space for a transient disturbance. The principle is used to derive a transformation law between a source spectrum and the resultant Doppler-shifted spectrum. The Doppler-shifted spectrum has a -3 power law in the spectral tail, the asymptotic behaviour of the tail is shown to be independent of the gravity-wave source. The result is obtained in two ways: from the gravity-wave energy equation and also by Fourier transforming the solution to the gravity-wave equations. The derived spectral transformation law should be a key point in spectral gravity-wave parametrizations.

KEYWORDS: Parametrization Transformation law

1. INTRODUCTION

Gravity-wave disturbances play an important role in determining the mean circulation. They can transport momentum from the lower atmosphere to higher levels, producing a forcing at the levels where they break or dissipate, that drives the circulation away from the radiative equilibrium. This forcing is indeed so strong that it is thought to be the main factor responsible for the inversion of the meridional temperature gradient in the mesosphere (e.g. Lindzen 1981).

Gravity waves are mainly generated in the troposphere and then propagate upwards. During their propagation the waves interact with the mean flow. The interactions can be classified into two large groups, reversible and irreversible interactions. The former produces a transient forcing on the mean flow, and as soon as the disturbance has passed the mean flow recovers its original state. On the other hand, the irreversible interactions produce changes in the mean flow which remain after the disturbance has passed that region.

Since small-scale gravity waves can not be resolved by general-circulation models, the irreversible interactions between the mean flow and the waves are taken into account in general-circulation models by means of parametrizations. A gravity-wave parametrization involves three main aspects of the waves, generation, propagation and dissipation.

Although attempts have been made to relate gravity-wave generation with probable sources (e.g. Charron and Manzini 2002), in general current non-orographic parametrizations do not use a physical approach to trigger gravity waves, but a climatological gravity-wave spectrum is specified at low altitudes.

The second aspect that a gravity-wave parametrization needs to represent is the gravity-wave propagation. The spectral parametrizations by Warner and McIntyre (1996, 2001) and Hines (1997) assume conservative *steady-state* propagation, so that the gravity-wave spectrum evolves following the conservation of the vertical wave-action flux (or alternatively, the so-called vertical pseudo-momentum flux, see McIntyre (1981)). In other words, under conservative steady-state propagation the vertical wave-action flux is the same *at any time and at any altitude*.

* Corresponding address: Department of Meteorology, The University of Reading, PO Box 243, Earley Gate, Reading RG6 6BB, UK. e-mail: m.a.pulido@rdg.ac.uk

The steady-state assumption is valid provided that gravity-wave sources are permanent and that there are no transient effects. However, sources in the atmosphere are highly transient. In general, high-resolution observations show that the envelope of oscillatory disturbances in space or time has a width of a few wavelengths or periods (e.g. Sato and Yamada 1994; Pavelin *et al.* 2001).

The third point that a gravity-wave parametrization needs to address is the physical process that dominates in a climatological sense the breaking or dissipation of the gravity-wave disturbances and therefore determines the form and intensity of the irreversible forcing to the mean flow.

Energy distributions derived from observations of horizontal wind and temperature show an apparent universal behaviour in short vertical wavelengths. The power spectrum has a -3 power law at high vertical wave number, and appears to be independent of the altitude, place and season (e.g. VanZandt 1982; Allen and Vincent 1995). There are several studies suggesting that the observed shape in the power spectrum is a manifestation of saturation produced by the dissipation or breaking of gravity waves (e.g. Dunkerton 1989).

A first attempt to explain the physical processes involved with the invariance of the power spectrum was made by Dewan and Good (1986). They associated the spectral tail to a non-interacting gravity-wave field which has a defined saturation amplitude for each vertical wave number given by the linear instability theory. This model has received strong criticisms by Hines (1991a).

Hines (1991b) has argued that the invariant shape in the spectrum is produced by the Doppler shifting of gravity waves by a statistical wave field. The high-wave-number part of the spectrum is Doppler shifted to vertical wave number $m = \infty$, i.e. the critical layer, where the gravity waves are eliminated by dissipative processes, while waves with lower wave number are contributing to the formation of the tail. This spectral tail resembles the observed characteristics of the spectrum in a limited range of vertical wave number but the results there are dependent on the source spectrum. In general, an asymptotic behaviour to a -1 power law is always found in Hines's model for every source spectrum.

It is important to note that nonlinear critical-layer interactions, proposed by Hines as the dominant saturation mechanism, are *not* the ones that determine the shape of the spectrum. The -1 power law is the result of the conservative propagation of gravity waves; specifically, the conservation of the vertical wave-action flux. On the other hand, the amplitude of the spectral tail is partially determined by critical-layer interactions.

In this paper, we focus on the conservative propagation of a general transient disturbance. The idea is to find the conservation laws in the spectral space for a transient disturbance. A transient disturbance does not conserve vertical wave-action flux for all times and for all altitudes. The quantity that is conserved for transient disturbances is the wave action which is *not* invariant for all times and for all altitudes, but it is conserved along the so-called ray tubes.

An illustration of a general transient disturbance is a gravity-wave packet. Since the wave activity in this case is concentrated in a spatio-temporal envelope, the vertical wave-action flux is changing with altitude and time. The limit for long time width of the envelope, and therefore for long altitude width, will lead to the steady state. As is well known, the spectral width is inversely proportional to the spatial width, so the steady-state limit in this case represents the monochromatic approximation in the spectral space.

The steady-state source assumption and thus vertical wave-action flux conservation has been used in earlier studies (Hines 1991b; Warner and McIntyre 1996) to derive a

spectral conservation law for vertical wave-number power spectra. It is worthwhile to investigate whether the so-found spectral transformation law for steady-state sources is also valid for transient sources.

It will be shown by two independent proofs that the conservation law in the wave-number space for transient disturbances is qualitatively different from the one obtained for steady-state disturbances.

Firstly, we derive an expression for a general disturbance that is propagating upwards in a non-rotating medium with a shear flow starting from the linearized Euler equations (section 2). The solution is expanded in horizontal wave number and absolute frequency since the mean flow is assumed to be uniform in horizontal coordinate x and t. By means of an analytical spectral analysis of the solution we find a transformation between the source spectrum and the Doppler-shifted spectrum. We show that for any source spectrum the resultant spectrum after Doppler shifting has a -3 power law in high vertical wave number (section 3(a)). These spectra are derived (Fourier transformed) from a time-fixed vertical profile which is the way that power spectra from observations are obtained and must be interpreted.

A second proof of the transformation law is derived starting from the wave-action conservation equation. As the disturbance propagates conservatively in a realistic background wind, *vertical profiles at different times conserve the total wave action* (the wave action integrated in space). A proof of this result is given in section 3(b). On the other hand, a comparison between two altitudes must conserve the vertical wave-action flux integrated in time.

Finally, in section 4, the theoretical results are confronted with a numerical experiment. A Gaussian wave packet is propagated in a background wind with vertical shear. The evolution of the wave packet shows that vertical profiles conserve the total wave action, while total vertical wave-action flux is not conserved. The power spectrum resulting from the numerical experiments agrees with the analytical power spectrum calculated from the spectral transformation law found in the theory.

2. Characteristics of the solution

Consider linear adiabatic perturbations in a non-rotating atmosphere consisting of an inviscid fluid, where the background conditions are given by a constant buoyancy frequency N and a horizontal wind $U(z)$, where z is height. Under the Boussinesq approximation, the resulting equation for the vertical velocity perturbation w is (e.g. Bretherton 1966; Booker and Bretherton 1967)

$$\mathrm{D}_{tt}\nabla^2 w - \mathrm{d}_{zz}U\mathrm{D}_t\partial_x w + N^2\partial_{xx}w = 0, \tag{1}$$

where $\mathrm{D}_t = (\partial_t + U\partial_x)$, $\partial_t = \partial/\partial t$, $\partial_x = \partial/\partial x$, $\mathrm{d}_z = \mathrm{d}/\mathrm{d}z$, with double subscripts denoting double derivatives.

Since the mean flow is uniform in x and t, we write the solution of (1) in the form

$$w(x, z, t) = w_1(z)\,\mathrm{e}^{\mathrm{i}(\omega t - kx)}, \tag{2}$$

where ω is the ground-based frequency and k the horizontal wave number. Substituting (2) in (1), the well-known Taylor–Goldstein equation is obtained:

$$\mathrm{d}_{zz}w_1 + \left\{\frac{N^2k^2}{(\omega - kU)^2} + \frac{k\mathrm{d}_{zz}U}{\omega - kU} - k^2\right\} w_1 = 0. \tag{3}$$

Equation (3) can be simplified taking usual approximations (Hines 1991b; Chimonas 1997). These are the hydrostatic approximation and to neglect the term related to the

curvature of the background wind. Under the hydrostatic approximation the perturbation field can be considered as quasi-horizontal (horizontal wind perturbation $u \gg w$) and therefore the $-k^2 w_1$ term can be neglected. Then, the resulting equation is

$$\mathrm{d}_{zz} w_1 + \frac{N^2 k^2}{(\omega - kU)^2} w_1 = 0. \tag{4}$$

We also assume that the characteristic distances for vertical changes are longer than one wavelength. This condition is satisfied for Richardson number much larger than 1/4, namely $Ri \equiv N^2 \mathrm{d}_z U^{-2} \gg 1/4$, which allows a solution in (4) using the WKB* method:

$$w(x, z, t) = w_0 \left(\frac{m_0}{m}\right)^{1/2} \mathrm{e}^{\mathrm{i}(\omega t - kx \pm \int_0^z m(z')\,\mathrm{d}z')}, \tag{5}$$

where w_0 is the wave amplitude, m_0 is the vertical wave number at the reference level that is assumed to be at $z = 0$, and m is the vertical wave number at z. The positive and negative signs indicate waves propagating upwards and downwards, respectively. To ensure that the above equation is a solution of (4), the following dispersion relation must be satisfied:

$$m^2 = \frac{k^2 N^2}{(\omega - U(z)k)^2}. \tag{6}$$

The so-found solution (5) is monochromatic in the sense that, at any given altitude, an observer sees a wave with a well-defined frequency and wave number. Obviously this is not the most general case. Actual sources are localized both spatially and temporally or, even if they are extended, they have non-periodic shapes which produce a wide spectrum of frequencies ω and wave numbers k and m.

The boundary conditions of the atmosphere (it does not have an upper limit) allow continuous modes, so the general solution is obtained through a double Fourier integral in ω and k:

$$w(x, z, t) = \frac{1}{2\pi} \iint \widetilde{w}(k, \omega) \left(\frac{m_0}{m}\right)^{1/2} \mathrm{e}^{\mathrm{i}(\omega t - kx + \int_0^z m\,\mathrm{d}z')}\,\mathrm{d}k\,\mathrm{d}\omega. \tag{7}$$

The function $\widetilde{w}(k, \omega)$ represents the spectral amplitude of the contributing waves. Note that, for the time being, $\widetilde{w}(k, \omega)$ is not the maximum amplitude of the vertical wind perturbation and by construction it is altitude independent.

The choice of only two spectral variables in (7) can be traced back to the existence of the dispersion relation (6). The fact that there is a dependence between wave number and frequency allows the use of only two of the three variables and, since the mean flow is non-uniform in z, the absolute frequency ω and horizontal wave number k are used as independent variables. A similar point of view was used by Zhu (1994), but he concentrated on the dissipation rather than Doppler-shifting effects.

The spectral amplitude can be obtained by Fourier transforming the velocity perturbation, $w(x, z, t)$, at the reference level ($z = 0$):

$$\widetilde{w}(k, \omega) = \frac{1}{2\pi} \iint w(x, 0, t)\, \mathrm{e}^{-\mathrm{i}(\omega t - kx)}\,\mathrm{d}x\,\mathrm{d}t. \tag{8}$$

The vertical velocity at $z = 0$, $w(x, 0, t)$, may be envisioned as the wave forcing at the boundary condition that is generating the disturbance.

* Wentzel–Kramers–Brillouin.

The phase average wave energy of the disturbance per unit volume is given by

$$W_r = \tfrac{1}{2}\rho_0(\overline{u^2} + \overline{w^2}) + \tfrac{1}{2}\rho_0 N^2 \overline{\zeta^2}, \tag{9}$$

where ρ_0 is the mean density, ζ is the vertical displacement ($D_t\zeta = w$), and overlines represent a phase average of the fields.

The first term of (9) is the kinetic energy of the disturbance and the second one is the potential energy. We use the principle of energy equipartition (Lighthill 1978) to express the wave energy as a function of velocity only:

$$W_r = \rho_0(\overline{u^2} + \overline{w^2}). \tag{10}$$

Since we are considering quasi-horizontal motions, the wave energy in this approximation becomes

$$W_r = \rho_0 \overline{u^2}. \tag{11}$$

We have found an expression of wave energy as a function of horizontal velocity perturbation only. Therefore, we derive the horizontal velocity perturbation from the mass conservation equation and the vertical velocity perturbation, (7):

$$u(x, z, t) = \frac{1}{2\pi} \iint \tilde{u}(k, \omega) \left(\frac{m}{m_0}\right)^{1/2} e^{i(\omega t - kx + \int_0^z m\, dz')}\, d\omega\, dk, \tag{12}$$

where $\tilde{u}(k, \omega) \equiv -(m_0/k)\tilde{w}(k, \omega)$ by definition. Assuming that $\tilde{u}(k, \omega)$ is known, the above equation gives the horizontal velocity perturbation at any place and time.

3. The vertical wave-number power spectrum

Waves in a fluid can exchange energy with the mean flow. In particular, when a wave disturbance propagates upwards in a shear flow the wave energy is not conserved. However, there is a quantity that is being conserved in the waves that is called the wave action (Bretherton and Garrett 1968; Lighthill 1978) defined as the wave energy density divided by the intrinsic frequency.

The wave-action conservation equation is coherent with each component of the solution (12); moreover, each component conserves the vertical component of its wave-action flux. Nevertheless, when a general transient disturbance is considered the vertical component of the wave-action flux at any fixed time is not conserved because the wave pattern is not stationary. This indicates that the spectral transformation law deduced from the conservation of the vertical component of the wave-action flux cannot be applied for a localized transient disturbance at a fixed time. In order to derive a transformation law, we examine the problem from two points of view: firstly, starting from the general solution and transforming the spectral domain in section 3(a); secondly, examining the wave-action conservation equation in section 3(b).

(*a*) *The transformation law derived from the general solution*

To examine the effects of Doppler shifting in the vertical wave-number power spectrum we compare a reference vertical wave-number power spectrum, which here is referred to as the source spectrum, with the resultant vertical wave-number power spectrum after Doppler shifting has taken place.

The source spectrum is the spectrum around the reference level; it may be identified as the spectrum at tropospheric altitudes. We calculate it by Fourier transforming the horizontal perturbation profile around $z = 0$. In the same way, the Doppler-shifted

spectrum is obtained by Fourier transforming the horizontal perturbation profile around $z = z_1$ where the background wind is $U = U(z_1)$.

In order to obtain the power spectrum as a function of the vertical wave number, we change variable in (12) from ω to m. The variable change is performed for a small enough altitude interval (say, $z_i = z_1 - L/2$ to $z_f = z_1 + L/2$) where the background wind U can be considered constant in a similar way to Hines (1991b) and Warner and McIntyre (1996); thus we take into account the changes produced by the background wind on the power spectrum below the interval in consideration. The calculated power spectrum represents the z_1 altitude (and its neighbourhood). Also note that the length of the interval L must be longer than the characteristic wavelength of the disturbance.

Then (12) is written within the interval from z_i to z_f as

$$u(x, z, t) = (2\pi L)^{-1/2} \iint \widetilde{u}(k, \omega(m)) \left(\frac{m}{m_0}\right)^{1/2} \mathrm{e}^{\mathrm{i}(\omega t - kx + m(z-z_i) + \alpha(m))} \partial_m \omega \, \mathrm{d}m \, \mathrm{d}k, \tag{13}$$

where $m = m(z_1; \omega)$ and $\alpha(m)$ is the phase of the mode at z_i. The 2-D Fourier transform in (k, m) is defined by

$$\widehat{F}(k, m) = (2\pi L)^{-1/2} \int_{-\infty}^{\infty} \int_{z_i}^{z_f} u(x, z, t) \, \mathrm{e}^{-\mathrm{i}(mz - kx)} \, \mathrm{d}x \, \mathrm{d}z. \tag{14}$$

Calculating the 2-D power spectrum (defined as the square of the absolute value of the Fourier transform) from (13), and taking into account that $\partial_m \omega = -Nkm^{-2}$, the resulting power spectrum is

$$|\widehat{F}(k, m)|^2 = |\widetilde{u}(k, \omega(m))|^2 \frac{N^2 k^2}{m_0 m^3}. \tag{15}$$

Integrating on the horizontal wave number in order to obtain the power spectrum only in terms of the vertical wave number, we obtain

$$|F(m)|^2 = \int |\widehat{F}(m, k)|^2 \, \mathrm{d}k = \frac{N^2}{m_0 m^3} \int k^2 |\widetilde{u}(k, \omega(m))|^2 \, \mathrm{d}k. \tag{16}$$

To find the power spectrum at the reference level $z = 0$, note that $m(z = 0, \omega) = m_0$, $U(0) = U_0$ and $N(0) = N_0$; then (16) becomes

$$|F_0(m_0)|^2 = \frac{N_0^2}{m_0^4} \int k^2 |\widetilde{u}(k, \omega(m_0))|^2 \, \mathrm{d}k, \tag{17}$$

where $|F_0|^2$ is the source spectrum. This spectrum is thought to be free of Doppler effects. Note that, depending on the characteristics of the problem in consideration, this spectrum may be regarded as the initial spectrum or the incident spectrum.

The relationship between the Doppler-shifted spectrum and the source spectrum is obtained replacing (17) in (16) and noting that $\tilde{u}$ is an altitude invariant quantity:

$$|F(m)|^2 = |F_0(m_0)|^2 \frac{N^2}{N_0^2} \frac{m_0^3}{m^3}. \tag{18}$$

Equation (18) can be regarded as a transformation law which relates the source spectrum amplitude to the amplitude that the mode has after the disturbance has suffered Doppler shifting by the relative background wind $\Delta U = U - U_0$.

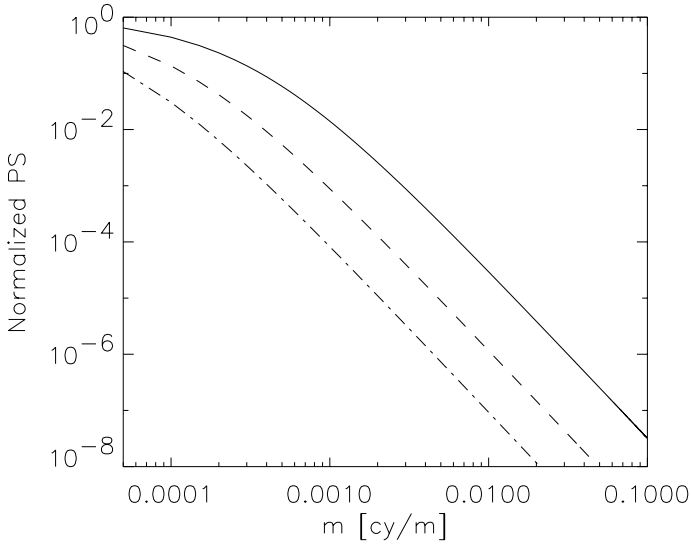

Figure 1. The Doppler-shifted spectrum of a constant source spectrum for different background winds: characteristic wave number $m_c = 2$ km^{-1} (continuous line), 0.7 km^{-1} (dashed) and 0.3 km^{-1} (dash-dot).

Taking into account the dispersion relation (6) and that the ground-based frequency and the horizontal wave number are constant during the propagation, the relationship between the vertical wave number at the reference level and the one at z_1 is

$$\frac{N_0}{m_0} = \Delta U + \frac{N}{m}. \tag{19}$$

Finally, changing variables in (18) from m_0 to m using (19), we obtain the power spectrum in a height interval characterized by a background wind U for an arbitrary source spectrum:

$$|F(m)|^2 = \left| F_0 \left(\frac{N_0}{\Delta U + N/m} \right) \right|^2 \frac{N_0}{N(1 + \Delta U m/N)^3}. \tag{20}$$

The power spectrum in (20) has a -3 power law at high wave numbers in agreement with observations. The spectral behaviour for high wave numbers is not altered by the shape of the source spectrum since the transformation (19) becomes wave-number independent for $m \gg N_0/\Delta U$ when it is assumed that the source spectrum contains intensities around the characteristic wave number, $m_c \equiv N/\Delta U$ (this assumption ensures the existence of the tail). On the other hand, the Doppler shifted spectrum for wave numbers lower than m_c depends on the original source spectrum. This is the part of the spectrum keeping some information about the sources. We will further deal with this in section 3(c).

Figure 1 shows a normalized constant source spectrum that is propagating in different background winds. The three curves are for $N = 0.02$ m s^{-1} and background winds of $\Delta U = 10$, 30 and 70 m s^{-1}. As the background wind increases, the amplitude of the spectral tail diminishes and the spectrum resembles the -3 power law at lower wave numbers.

(*b*) *The transformation law derived from wave-action conservation*

We now derive the conservation principle that governs the spectral transformation law (18). We start from the equation of wave-action conservation (Lighthill 1978):

$$\partial_t \frac{W_\mathrm{r}}{\Omega} + \nabla \cdot \left(\frac{W_\mathrm{r}}{\Omega} \mathbf{c}_\mathrm{g} \right) = 0, \tag{21}$$

where Ω, the intrinsic frequency, is the frequency relative to the background wind ($\Omega = \omega - kU$), $\mathbf{c}_\mathrm{g}$ is the group velocity vector, and $W_\mathrm{r} = W_\mathrm{r}(x, z, t)$ is the wave energy density. Equation (21) establishes that the wave action is transported conservatively along the path traced by the disturbance.

In what follows, we assume a wave packet with a fixed horizontal wave number. If it were not the case, an integration in x must be performed and W_r must be interpreted as $W_\mathrm{r}(z, t) = (2\pi)^{-1} \int_{-\infty}^{\infty} W_\mathrm{r}(x, z, t)\, \mathrm{d}x$. In any case, (21) is reduced to

$$\partial_t \frac{W_\mathrm{r}}{\Omega} + \partial_z \left(\frac{W_\mathrm{r}}{\Omega} c_{\mathrm{g}z} \right) = 0. \tag{22}$$

Now we integrate in altitude at a fixed time, the altitude interval is chosen to be long enough to ensure the complete disturbance is inside it:

$$\partial_t \int_{z_i}^{z_f} \frac{W_\mathrm{r}}{\Omega}\, \mathrm{d}z + \left(\frac{W_\mathrm{r}}{\Omega} c_{\mathrm{g}z} \right) \Big|_{z_i}^{z_f} = 0. \tag{23}$$

As the wave energy density is zero at the extremes, the resulting equation is

$$\partial_t \int_{z_i}^{z_f} \frac{W_\mathrm{r}}{\Omega}\, \mathrm{d}z = 0. \tag{24}$$

This expression shows that *vertical profiles for a general disturbance conserve the wave action*. In other words, if the total wave action of two vertical profiles at different times are compared, they are equal.

Density changes with altitude do not affect the shape of the spectrum, they only increase the amplitude uniformly, therefore they are not taken into account. Using the Parseval theorem and replacing (11), we obtain

$$\int_{z_i}^{z_f} \frac{\overline{u^2}}{\Omega}\, \mathrm{d}z = \frac{1}{2} \int \frac{|F(m)|^2}{\Omega}\, \mathrm{d}m = \text{constant}. \tag{25}$$

We compare two vertical profiles at different times, one where the disturbance is located in the reference background wind and the other when, after an upward propagation, the disturbance is located in a background wind U. Besides, we use the dispersion relation (6) so the power spectra are related by

$$\int \frac{m}{N} |F(m)|^2\, \mathrm{d}m = \int \frac{m_0}{N_0} |F(m_0)|^2\, \mathrm{d}m_0. \tag{26}$$

The integration variable on the right-hand side is transformed from m_0 to m, and note that $\mathrm{d}m_0/\mathrm{d}m = m_0^2/m^2$ from (19). Then the power spectral amplitudes are related by

$$|F(m)|^2 = |F_0(m_0)|^2 \frac{N^2\, m_0^3}{N_0^2\, m^3}. \tag{27}$$

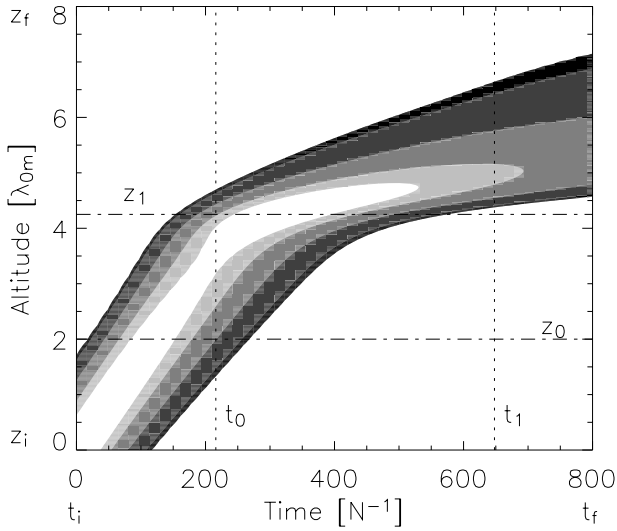

Figure 2. Wave energy per unit mass of a disturbance propagating upwards. Lighter contours show higher wave energy (contours are 0.075, 0.1, 0.25, 0.5 and 0.75). Horizontal and vertical straight lines show the path of integration (see text for details).

Therefore, we recover the transformation law obtained in (18).

An illustration of the differences between the wave action and the vertical flux invariance can be seen in Fig. 2, which shows the path of the envelope (wave energy density) of a disturbance which is propagating conservatively upwards (see details in section 4). The total wave action observed by a radiosonde launched at time t_0 which measures from z_i to z_f is the same as that measured by a radiosonde launched at t_1; the power spectra are related by the derived transformation law (27).

On the other hand, if we measure the perturbation of the disturbance at fixed altitudes (say z_0, and z_1) during the entire passage of the disturbance, for instance from t_i to t_f (see Fig. 2), the vertical wave-action flux integrated in time is height invariant. This results from (22), which, integrated in time between t_i and t_f, gives $\partial_z \int_{t_i}^{t_f} (W_\mathrm{r}/\Omega) c_{\mathrm{g}z}\, \mathrm{d}t = 0$. If we want to examine the disturbance from the spectral point of view in this case we will have frequency power spectra but not vertical wave-number power spectra. These frequency power spectra will conserve vertical momentum flux.

In the case of a monochromatic event, the wave pattern is stationary and the first term of (21) is zero since, obviously, a monochromatic wave has a fixed wave frequency. Therefore monochromatic waves conserve the vertical wave-action flux even for a fixed time profile. They are expected to have a different spectral behaviour (Pulido and Caranti 2000). These events are sporadic because they require a source that excites a single mode and also the source excites it for a long time. Even topographic waves, if they are generated by a non-steady incident flow, have a broad frequency spectrum (Lott and Teitelbaum 1993).

(*c*) *The source spectrum influence*

Figure 3 shows a curve representing the relation between a wave number in a background wind U_0 and the wave number refracted by an environment where the characteristic wave number is m_c (defined in section 3(a) as $N_0 \Delta U^{-1}$). The strongest effect is observed at incident wave numbers belonging to the neighbourhood of m_c

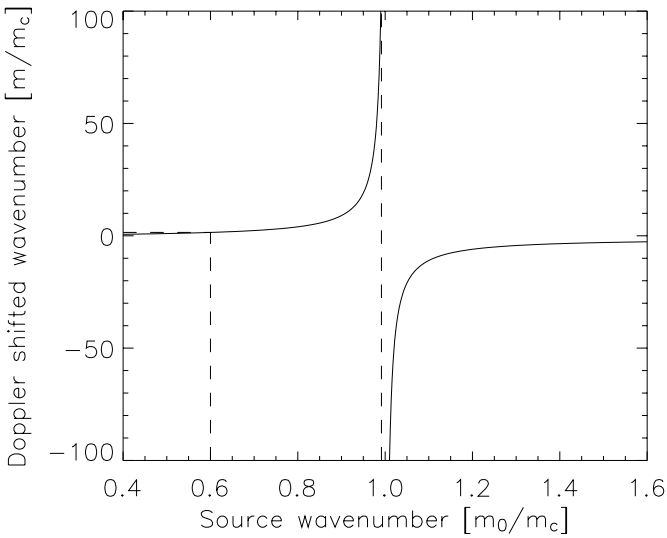

Figure 3. The refracted wave number m as a function of the incident wave number m_0 (see text). Note the difference of axis scales. For a monotonic mean wind, waves with $m_0 > m_c$ should be interpreted as absorbed waves through critical layers instead of Doppler shifting to negative values.

which after Doppler shifting will produce the spectral tail. Thus, the more refracted the wave packets are, the less monochromatic their characteristics will be. The latter fact contributes to justify our approach of using a continuous spectrum instead of monochromatic waves.

We would like to point out that any power law in the source spectrum results after Doppler shifting in the same -3 slope. In fact, let us take a spectrum of the shape $|F_0(m_0)|^2 = am_0^p$. Clearly, for p positive (negative), high (low) wave numbers are dominant. The resulting power spectrum is

$$|F(m)|^2 = \frac{a}{m^3(1/m_c + 1/m)^{3+p}}. \tag{28}$$

The -3 power law is recovered for high wave numbers ($m > m_c$). In particular, if the source spectrum already has a -3 slope, this spectrum is conserved under the Doppler shifting. Moreover, the amplitude of the tail is also conserved. This means that the transformation is transparent to the -3 power law*.

To illustrate the independence of the source spectra, Fig. 4 shows the Doppler-shifted power spectra for three source power spectra (a constant power spectrum, a -1 power law, and $+1$ power law). These power spectra have exactly the same asymptotic -3 power law.

The Doppler-shifted spectral tail is composed of waves that originally were within the range $m_c/2 < m_0 < m_c$. The lower limit goes to m_c in the Doppler-shifted spectrum which marks the division between the low-wave-number spectral region, where a general behaviour is not defined by Doppler shifting (it depends on the sources), and the spectral tail, which has a completely determined power law given by Doppler shifting.

* Figure 1 apparently contradicts this fact since there are different amplitudes for different winds. The wave spectrum that reaches, say, a wind U and already presents a slope -3 should not be further altered but Fig. 1 suggests it is. An explanation is found in the behaviour of wave numbers in the neighbourhood of m_c. If there the slope is already -3 then the spectrum is transparent to the Doppler shifting. However, the spectra shown in Fig. 1, which come from a constant spectrum, nearby m_c never have -3 slope and therefore they are altered.

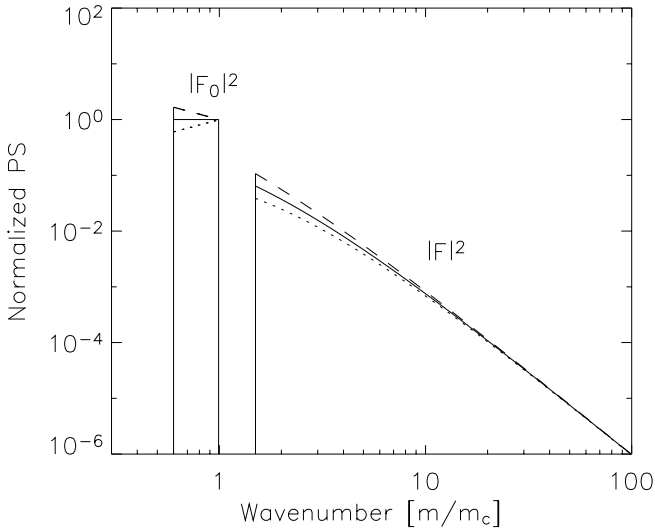

Figure 4. Source power spectra $F_0^2 = A$ (solid line), $|F_0|^2 = Am_0$ (dotted line) and $|F_0|^2 = Am_0^{-1}$ (dashed line), and the corresponding Doppler-shifted power spectra. The wave-number ranges are shown with a dashed line in Fig. 3. See text for explanation.

If the mean wind profile is monotonic with altitude from $U(0) = 0$ at the reference level to $U(z_1) > 0$ at the observation point, it is expected that waves contained in the source spectrum with wave number higher than m_c are eliminated through absorption in the corresponding critical layer. Thus one can think of Doppler shifting as a 'transporting' process from the high to the small scale. The elimination of modes does not alter the shape in the high-wave-number part of the Doppler-shifted power spectrum, it just imposes a high-cut wave number in the *source* spectrum (note this entity evolves in time, and could be misinterpreted with the term 'initial' spectrum), the modes lower than this maximum wave number m_c will produce a full spectral tail with a -3 power law.

There is an implicit approximation in the picture: there should be no effects on the wave numbers below m_c in the original spectrum; however, waves in the immediate left neighbourhood of m_c are probably being altered, among other things, by dissipation and by degradation into turbulence during the propagation up to the observation point. With respect to the tail region in the resultant spectrum, we may consider that, within an interval from m_c to some wave number m_M, the spectrum is dominated by conservative Doppler shifting and beyond m_M the effects of turbulence and dissipation start prevailing.

4. Numerical simulation

In this section a numerical linear study of the propagation of a continuous spectrum of waves on a shear background wind is presented. The objective is to compare the numerical results with the theory in order to test the analytical results obtained in section 3. The study is also an illustration of the mechanisms involved in non-steady disturbances.

The numerical model solves (1) using the spectral method in x and t (Durran 1999) while the resulting second-order equation in z, (3), is represented by two first-order

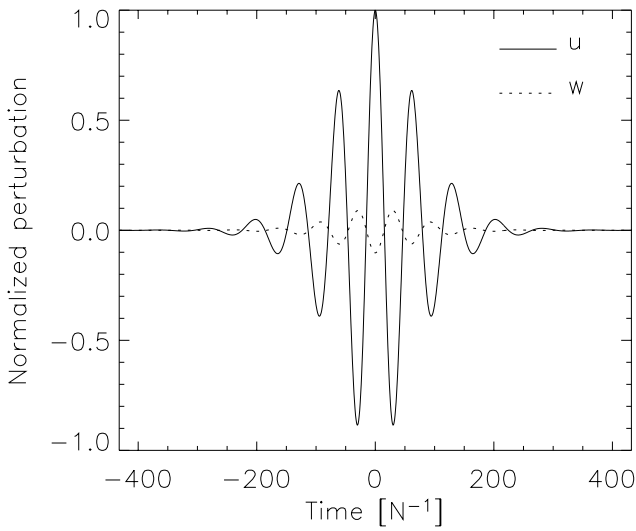

Figure 5. Bottom boundary conditions at level $z = 0$: horizontal perturbation (solid line) and vertical perturbation (dotted line).

equations for horizontal and vertical velocities which are solved using a fourth-order Runge–Kutta method with adaptative step size (Press *et al.* 1992). With the numerical model we can test the analytical derivation and also the validity of the approximations which lead from (3) to (4).

Consider that a source of gravity waves located in $z = 0$ radiates a Gaussian spectrum given by

$$F_0(m_0) = \frac{1}{(2\pi)^{1/2}\sigma}\, \mathrm{e}^{-(2\sigma^2)^{-1}(m_0 - m_{0\mathrm{m}})^2}, \tag{29}$$

where $m_{0\mathrm{m}}$ is the central wave number and σ is the width of the spectrum. We assume that the disturbance is periodic in x.

The problem can be thought of as a membrane located in the horizontal plane, $z = 0$ (lower boundary) which is vibrating and generating perturbations. The horizontal and vertical velocity at the bottom boundary $z = 0$ as a function of time are shown in Fig. 5. Since the fields are continuous and the source is emitting at $z = 0$, we impose the radiation condition as upper boundary to allow only upgoing waves.

Once the spectrum is radiated from the source about $t = 0$, it starts propagating upwards in a medium that is characterized by a constant Brunt–Vaïsälä frequency and background wind with a hyperbolic tangent profile

$$U = \frac{U_m}{2}[1 + \tanh\{\Gamma(z - z_{\mathrm{s}})\}]. \tag{30}$$

This background wind profile (30) has ideal characteristics for studying the Doppler effect. There, three regions can be identified (see Fig. 6): an almost constant wind, $U = 0$, for low altitudes ($z < z_{\mathrm{s}}$), a shear layer with a linear wind about z_{s} and smooth transitions to the other layers, and a third layer at high altitudes with a background wind $U = U_m$.

To diminish the number of free parameters, $\lambda_{0\mathrm{m}} = 2\pi/m_{0\mathrm{m}}$ and N^{-1} are taken as longitude and time units, respectively. For this numerical study case, the wave packet is

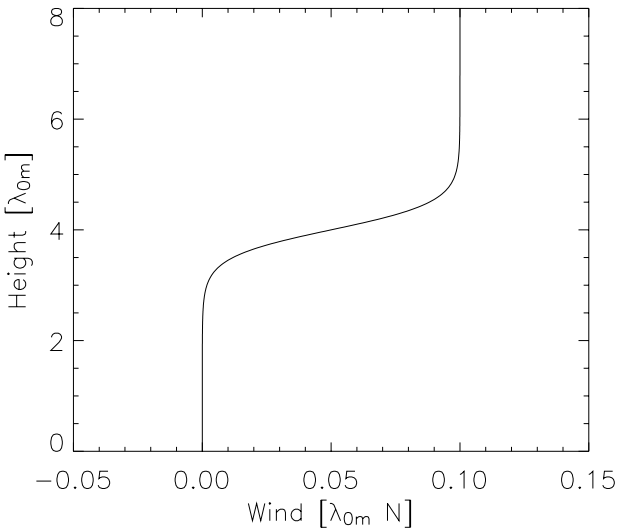

Figure 6. Background wind. The units are explained in the text.

characterized by $\sigma = 0.15m_{0\mathrm{m}}$ and $k = 0.1m_{0\mathrm{m}}$. The background wind parameters are chosen to be $z_{\mathrm{s}} = 4\lambda_{0\mathrm{m}}$, and $U_m = 0.1N\lambda_{0\mathrm{m}}$, the maximum vertical shear is such that the minimum Richardson number is 100. Taking typical values $N = 0.02\ \mathrm{s}^{-1}$, $\lambda_{0\mathrm{m}} = 5$ km, the maximum background wind would be $U_m = 10\ \mathrm{m\ s}^{-1}$. In practice, the numerical experiments are performed with the bottom boundary at $z = -3\lambda_{0\mathrm{m}}$ so that we can examine the whole envelope at $t = 0$.

The vertical profiles of the horizontal perturbation at the initial time and after Doppler shifting has taken place at $t = 1000N^{-1}$ are shown in Fig. 7. Even when the wave packet is propagating towards the critical layer (the vertical wave number is increasing), the amplitude of the perturbations are diminishing.

The differences between the vertical profiles calculated with the approximate equation, (4), and with the exact Taylor–Goldstein equation (3) are lower than 3%. As expected these differences diminish for higher vertical wave numbers.

Figure 8 shows the wave energy density as a function of z for different times; when the wave packet is located entirely above the shear layer the envelope has lost its Gaussian shape due to dispersion and Doppler shifting. In particular, it is not symmetrical—the upper part is broader than the lower part. The wave energy density as a function of z and t is shown in Fig. 2, note that the maximum amplitude of the envelope decreases with time.

The integral over the altitude interval of wave energy density, wave action and the vertical component of momentum flux are shown in Fig. 9. Since a periodic forcing in the horizontal is assumed, the integral of wave energy can also be interpreted as the wave energy per horizontal longitude unit. Because the wave packet is refracting towards higher vertical wavelengths (lower relative frequency) the wave energy is decreasing as the time goes on, as clearly seen in Fig. 9. The same feature is observed for the vertical momentum flux. Thus, in complete agreement with the theoretical analysis, *the total vertical momentum flux is not conserved in vertical profiles*: it is diminishing when there is Doppler shifting towards higher wave number. On the other hand, the total wave action is conserved. As already mentioned, this means that if we launch two radiosondes

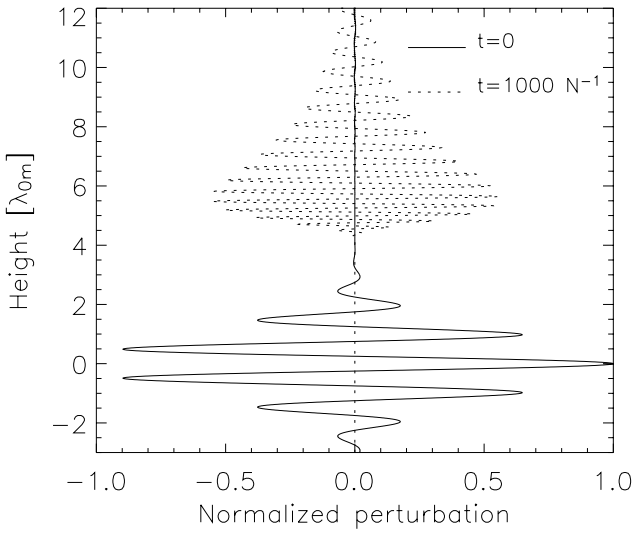

Figure 7. Horizontal perturbation at $t = 0$ (solid line) and after the disturbance has been Doppler shifted by the shear layer at $t = 1000N^{-1}$ (dotted line).

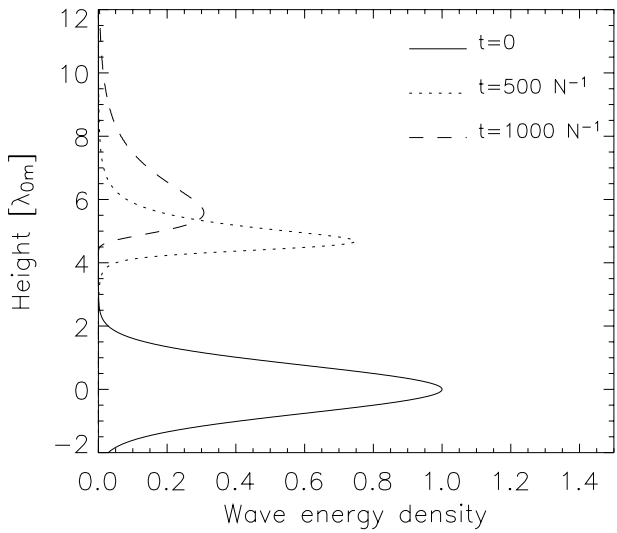

Figure 8. Normalized wave energy density profiles at different times.

at different times, the measured vertical profiles and their power spectra conserve wave action.

Different behaviour would be found with a sonde measuring, *at a fixed altitude*, the complete passage of the disturbance as the time goes on. In this case, shown in Fig. 10, the vertical momentum flux integrated in time is conserved so that its divergence vanishes, while wave action and wave-momentum flux integrated in time are increasing when the disturbance is suffering Doppler shifting towards higher wave numbers. The temporal width of the wave packet is widening with Doppler shifting, so if we were measuring with the fixed altitude sonde, it would be necessary to measure a very long

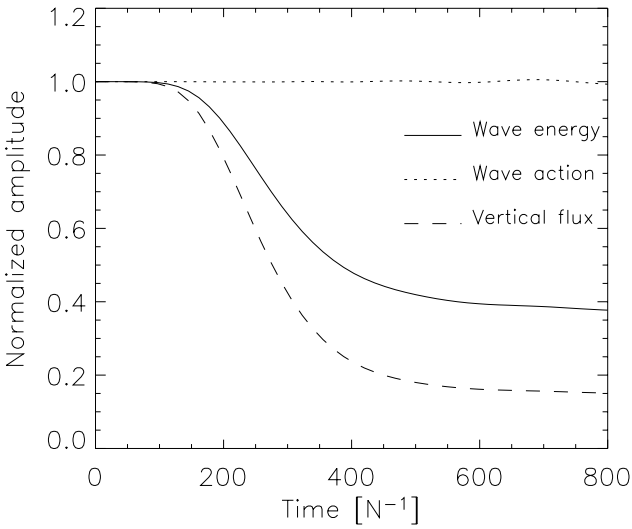

Figure 9. Evolution of the total wave energy, total wave action and total vertical wave-action flux.

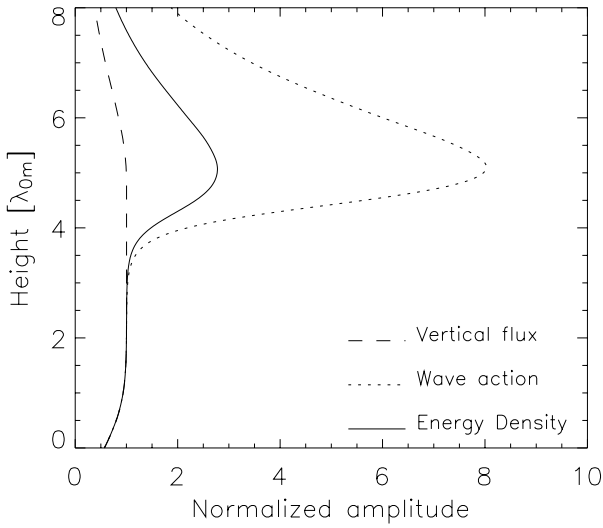

Figure 10. Profiles in height z of the wave energy density, wave-action density and vertical wave-action flux integrated in time.

time (the temporal width is infinity at the critical level since group velocity goes to zero) to satisfy the conservation of the integral in time of vertical momentum flux. In fact, the divergences of vertical flux that are observed at high altitudes in Fig. 10 are because the disturbance (say the lower part of the envelope) is still at those altitudes at the upper limit of time considered in the integration.

The validity of the derived spectral law (20) is readily tested. Vertical profiles of the disturbance at different times are numerically Fourier transformed to get the power spectrum; this numerical power spectrum is compared with the predicted one from the theoretical transformation law.

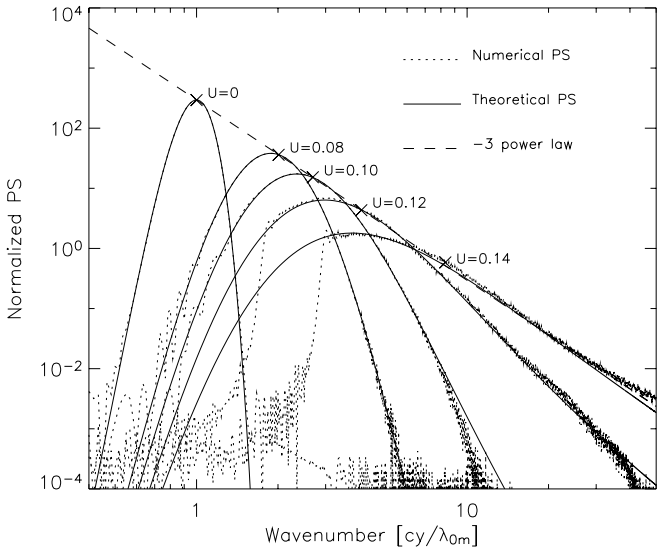

Figure 11. Power spectra for different background winds: $U = 0$, 0.08, 0.1, 0.12 and 0.14 $N\lambda_{0\mathrm{m}}$. Crosses indicate the central wave number. The -3 power law is also shown (dashed line).

Figure 11 presents the numerical power spectra (dotted lines) resulting from the propagation of the disturbance (29) at different background winds defined by (30). The analytical power spectra from (20) (continuous lines) are also shown in Fig. 11. The numerical power spectra agree rather well with the theoretical ones for any background wind.

Figure 11 shows two features of the transformation law. The first feature is that the amplitudes of a component of the spectrum at different background winds are related by (20). Note the crosses in Fig. 11 showing the amplitude of the central wave number for different background winds which fits almost exactly the -3 straight line (dashed line). The other feature shown in the theory was the appearance of a spectral tail with a -3 power law when the source power spectrum has amplitudes near the wave number m_{c}. Figure 11 shows the Doppler-shifted power spectrum by a background wind of $U = 0.14N\lambda_{0\mathrm{m}}$, which is of the order of the smallest phase speed of the packet, $N(m_{0\mathrm{m}} - \sigma)^{-1}$. This spectrum presents the asymptotic behaviour characteristic of the transformation law which produces a spectral tail with a -3 power law.

5. Discussion and conclusions

Perhaps the most important conclusion is the realization that there are profound differences when using monochromatic or continuous source spectra in the resulting vertical wave-number spectrum. These differences can be ascribed to the interference between components in the continuous case leading to a -3 spectral tail while the monochromatic one, free of such interference effects, gives a -1 tail. These interference effects are directly related to the fact that the vertical wave number can not be considered a spectral variable from a mathematical point of view: different bins (modes) interchange energy in this space even in this linear problem and therefore amplitudes of bins in this space can not be considered time independent. The only case where the amplitudes are time independent is in a monochromatic wave because it has a stationary pattern in the physical space.

Although there are previous works that examine the Doppler effect (Hines 1991b; Warner and McIntyre 1996), they are based on the vertical wave-action flux conservation. The spectral conservation law obtained in those works can only be used for permanent gravity-wave sources. Gravity-wave parametrizations must use the derived transformation law (18) in order to evolve the source power spectrum, specially those parametrizations which pretend to represent highly transient and intermittent sources (e.g. convection, fronts) as well as parametrizations with stochastic sources.

If transient phenomena are represented by the assumption of vertical wave-action flux conservation, this assumption leads to an overestimation of the amplitudes at high vertical wave-number modes, which in turn results in unrealistic momentum flux deposition at low altitudes. Furthermore, the wave energy increases with Doppler shifting towards higher vertical wave number for a steady-state disturbance. On the other hand, for a transient disturbance the wave energy decreases with Doppler shifting towards higher vertical wave number. The representation of transient phenomena in gravity-wave parametrizations and the differences with the steady-state representation will be addressed in a future work. The results for transient disturbances obtained here can be applied directly in current gravity-wave parametrizations since the derivation follows the main gravity-wave assumptions, the hydrostatic approximation and a non-rotating medium, taken in current spectral schemes (e.g. Hines 1997; Warner and McIntyre 2001).

The resultant Doppler-shifted spectrum does not depend on the shape of the source spectrum. As long as there are waves around m_c, there will be a -3 tail after Doppler shifting.

So far the -3 power law and the saturation of the wave field have been identified in the literature as a manifestation of the same physical process; however, following the results of this work, they can be independent features. A direct example of this fact is that there can appear observed power spectra with a power law close to -3 which are saturated or unsaturated and the shape is only a manifestation of a wave field with linear and conservative propagation.

For a saturated wave field the conservative Doppler shifting could be carrying part of the energy to high vertical wave number and also regulating the amount of energy that is available to be dissipated in the critical layer. In this case, the Doppler shifting could be determining the spectral tail in the observed spectral range while dissipative processes related with the critical layer could be dominant at higher vertical wave number. However, dissipative and nonlinear processes could also be playing a role in the same spectral range specially at the highest vertical wave-number part. Since we have only considered linear and conservative propagation we can not evaluate the relative importance of dissipation and nonlinearities with the present model.

Acknowledgements

The author thanks G. Chimonas, J. Thuburn, an anonymous reviewer and the associate editor for helpful comments.

References

Allen, S. J. and Vincent, R. A. 1995 Gravity wave activity in the lower atmosphere: Seasonal and latitudinal variations. *J. Geophys. Res.*, **100,** 1327–1350

Booker, J. and Bretherton, F. 1967 The critical layer for internal gravity waves in a shear flow. *J. Fluid. Mech.*, **27,** 513–539

Bretherton, F. 1966 The propagation of groups of internal waves in a shear flow. *Q. J. R. Meteorol. Soc.*, **92,** 466–480

Bretherton, F. and Garrett, C. 1968 Wavetrains in inhomogeneous moving media. *Proc. R. Soc. A*, **302,** 529–554

Charron, M. and Manzini, E. 2002 Gravity waves from fronts: Parameterization and middle atmosphere response in a general circulation model. *J. Atmos. Sci.*, **59,** 923–941

Chimonas, G. 1997 Waves and the middle atmosphere wind irregularities. *J. Atmos. Sci.*, **54,** 2115–2128

Dewan, E. M. and Good, R. E. 1986 Saturation and the 'universal' spectrum for vertical profiles of horizontal scalar winds in the atmosphere. *J. Geophys. Res.*, **91,** 2742–2748

Dunkerton, T. 1989 Theory of internal gravity wave saturation. *Pure and Applied Geophys.*, **130,** 373–397

Durran, D. R. 1999 *Numerical methods for wave equations in geophysical fluid dynamics*. Springer-Verlag, Heidelberg, Germany

Hines, C. O. 1991a The saturation of gravity waves in the middle atmosphere. Part I: Critique of linear-instability theory. *J. Atmos. Sci.*, **48,** 1348–1359

1991b The saturation of gravity waves in the middle atmosphere. Part II: Development of Doppler-spread theory. *J. Atmos. Sci.*, **48,** 1360–1379

1997 Doppler spread parametrization of gravity-wave momentum deposition in the middle atmosphere. Part 1: Basic formulation. *J. Atmos. Sol. Terr. Phys.*, **59,** 371–386

Lighthill, J. 1978 *Waves in fluids*. Cambridge University Press

Lindzen, R. S. 1981 Turbulence and stress owing to gravity wave and tidal breakdown. *J. Geophys. Res.*, **86,** 9707–9714

Lott, F. and Teitelbaum, H. 1993 Topographic waves generated by a transient wind. *J. Atmos. Sci.*, **50,** 2607–2624

McIntyre, M. E. 1981 On the 'wave momentum' myth. *J. Fluid Mech.*, **106,** 331–347

Pavelin, E., Whiteway, J. A. and Vaughan, G. 2001 Observation of gravity wave generation and breaking in the lowermost stratosphere. *J. Geophys. Res.*, **106,** 5173–5179

Press, W. H., Flannery, B. P., Teukolsky, S. A. and Vetterling, W. T. 1992 *Numerical recipes in Fortran*. Cambridge University Press

Pulido, M. and Caranti, G. 2000 Power spectrum of a gravity wave propagating in a shearing background. *Geophys. Res. Lett.*, **27,** 101–104

Sato, K. and Yamada, M. 1994 Vertical structure of atmospheric gravity waves revealed by the wavelet analysis. *J. Geophys. Res.*, **99,** 20623–20631

VanZandt, T. E. 1982 A universal spectrum of buoyancy waves in the atmosphere. *Geophys. Res. Lett.*, **9,** 575–578

Warner, C. D. and McIntyre, M. E. 1996 On the propagation and dissipation of gravity wave spectra through a realistic middle atmosphere, *J. Atmos. Sci.*, **53,** 3213–3235

2001 An ultrasimple spectral parameterization for nonorographic gravity waves. *J. Atmos. Sci.*. **58,** 1837–1857

Zhu, X. 1994 A new theory of the saturated gravity wave spectrum for the middle atmosphere. *J. Atmos. Sci.*, **51,** 3615–3625